Soil Dynamics and Earthquake Engineering 128 (2020) 105866

Contents lists available at ScienceDirect

Soil Dynamics and Earthquake Engineering

journal homepage: www.elsevier.com/locate/soildyn

Uniform damping ratio-based design method for seismic retrofitting of elastoplastic RC structures using viscoelastic dampers

Liyu Xie[a], Li Zhang[a], Chao Pan[b], Ruifu Zhang[a,*], Tianli Chen[c]

[a] Department of Disaster Mitigation for Structures, Tongji University, Shanghai, 200092, China
[b] College of Civil Engineering, Yantai University, Yantai, 264005, China
[c] School of Civil Engineering, Xi'an University of Architecture and Technology, Xi'an, 710055, China

ARTICLE INFO

Keywords:
Uniform damping ratio
Seismic retrofit
Viscoelastic damper
Energy dissipation

ABSTRACT

A simple design procedure is proposed for seismic retrofitting of existing structures using viscoelastic dampers (VEDs) based on the uniform damping ratio (UDR) concept to make full use of each damper. The UDR concept states that the equivalent damping ratios, which represent the energy dissipation capacities of the dampers, are the same for each installed VED. The stiffness and damping characteristic parameters of the damped structure can be formally decoupled using UDR-based derivations, which simplify the determination of the VEDs' parameters. The generalized single-degree-of-freedom method and pushover analysis are adopted for a fast estimation of the seismic response of the damped elastoplastic structure. Taking the response reduction ratio as the design target, a seismic retrofit design procedure is proposed based on the UDR concept to meet the performance demand. Finally, a six-story frame is adopted to illustrate the proposed design method. The dynamic analysis results show that the seismic responses of the structure are well-controlled, as expected, and that the installed VEDs are used effectively. The conclusion can be drawn that the UDR-based design method for retrofitting an existing structure using VEDs is rational and effective.

1. Introduction

In the past few decades, the application of passive energy dissipation technology has been of great interest to many engineers and scholars for seismic risk mitigation in building structures [1–3]. Using energy dissipation devices (EDDs), the energy caused by earthquakes can be effectively absorbed and dissipated for structures with suitably placed dampers, and the reliability of the structures can be enhanced [1,4–7]. Therefore, the use of EDDs has increased substantially for the seismic retrofitting of structures. While some theories and methods have been presented for this technology, more detailed and deeper studies are still needed for the seismic retrofitting of existing structures with EDDs [2,8–10]. This is because, compared with the application of EDDs for new structures, the seismic retrofitting of structures using EDDs involves the original characteristics of the existing structures, making this process more difficult.

This study is mainly focused on the viscoelastic damper (VED), which was one of the earliest devices used as an EDD for structural response control [11–13]. These dampers are characterized by frequency and temperature dependence and the energy is dissipated through the shear deformation of the corresponding viscoelastic materials (e.g., polymeric material, rubber material, etc.). With the advantages of low cost, simple implementation, adding both damping and stiffness and activating at low displacements, VEDs are popular for structural retrofits to control wind and seismic responses [14–16]. The dynamic behaviors of VEDs are usually described using the classic rheological models (simple/generalized Kelvin and Maxwell model) and fractional derivative models [17–20]. Among these models, the classic rheological models are more often used in practice for the analysis and design of structural seismic retrofitting [17].

A simple, effective and reasonable design method is very important for the application of structural seismic retrofitting using VEDs. This process usually involves the determination of the VED's locations and parameters (i.e., the storage stiffness, K'_d, the loss stiffness, K''_d and the loss factor, $\eta_d = K''_d/K'_d$, etc.). For these purposes, numerous design methods have been suggested for structures with supplemental VEDs. In early VED applications, Zhang and Soong [13] proposed design procedures based on the control index, resulting in a sequential procedure for obtaining the optimal locations for VEDs. However, the structure is equipped with uniform dampers in this method, which cannot fully utilize these dampers. For seismic retrofit designs, Lee et al. [21] proposed a simplified design procedure for frame buildings using VEDs,

* Corresponding author.
E-mail address: zhangruifu@tongji.edu.cn (R. Zhang).

https://doi.org/10.1016/j.soildyn.2019.105866
Received 10 May 2019; Received in revised form 9 August 2019; Accepted 18 September 2019

and the stiffnesses of the VEDs installed at each story are determined using a trial calculation procedure. The design methods mentioned above are presented on the basis of assumed elastic structures. However, under strong ground motions, plastic behavior can occur in the primary structures. Hence, these design methods may not be reliable when the primary structures move into the plastic stage. Mazza and Vulcano [22] suggested a displacement-based design procedure for elastoplastic RC framed buildings using damped braces. Zhang et al. [23] presented the direct design method of VED parameters for damped structures based on the elastic-plastic response reduction curve, which is an extension for the research of the Japan Society of Seismic Isolation [24]. However, this curve is not easy to plot. Joaquim and Zhou [25] suggested a practical design method for new and retrofit buildings, obtaining the VED parameters using the shear forces instead of the story stiffnesses of the original structures, and the placement of the VEDs are determined according to the sequential procedure presented by Zhang and Soong [13]. With the objective of determining the optimal placement of VEDs and minimizing the cost, many optimal design methods are also presented by scholars using different algorithms. Fujita et al. [26] presented a gradient-based optimization methodology to obtain the optimal placement of VEDs. A genetic algorithm is employed by Zhao et al. [27] to optimally place the VEDs under a determined amount of viscoelastic material. Shmerling et al. [28] presented a robust analysis redesign iterative approach for the optimal seismic retrofit design of structures using dampers with the objective function of minimizing the cost. However, the complexity of the corresponding algorithms limited the application of these optimal methodologies in practice. To sum up, there is still a need to propose simple, effective, and reasonable design procedures for the seismic retrofit of structures using VEDs.

The uniform damping ratio (UDR) concept [29] is recommended for the seismic retrofit design of the structures in this study, which means that the equivalent damping ratios provided by the VEDs are equal for each story of the structure. This concept is presented to sufficiently utilize the VEDs, as the energy dissipation capacity of the VED is measured by the equivalent damping ratio. According to the UDR concept, the equation for the additional damping ratio is derived in which the added stiffness and damping effect of the VEDs are uncoupled, which makes the corresponding design procedure simpler. Additionally, it has been proven that the uncoupled stiffness characteristic parameter can be used to proportionally determine the storage stiffness of the supplemental VEDs, which can make the vibration mode shapes of the structure almost unchanged when the VEDs are installed [15]. This situation is usually expected for the seismic retrofit of a structure. Furthermore, using the generalized single-degree-of-freedom (SDOF) model and considering the elastic-plastic behavior of the primary structure, the seismic retrofit design procedures are presented that meet seismic performance demands of the assumed earthquake intensity. Finally, a six-story RC frame is used to illustrate the design method, and a time history analysis is performed for verification.

2. Illustration of the design theory

2.1. Details of the UDR concept

It is usually expected that all the dampers that are installed at the structure can work fully under dynamic loads. The energy dissipation capacity of a VED can be determined using the parameter of the equivalent damping ratio. Hence, to equally use all the dampers, the UDR concept is suggested, which assumes that the equivalent damping ratio of each installed VED at the structure is the same. The equivalent damping ratio of a VED, $\zeta_{d,i}$, can be expressed as follows [30]:

$$\zeta_{d,i} = \frac{E_{d,i}}{4\pi E_{sd,i}} \tag{1}$$

where $E_{d,i}$ is the energy dissipated in one cycle by the ith equipped VED and $E_{sd,i}$ is the maximum strain energy of the ith VED in the same cycle.

When the dampers are installed at the structures, the additional damping ratio of the dampers, ζ_a, can be calculated as follows:

$$\zeta_a = \frac{\sum E_{d,i}}{4\pi E_{sa}} = \frac{\sum E_{d,i}}{4\pi \sum E_{sd,i}} \cdot \frac{\sum E_{sd,i}}{E_s + \sum E_{sd,i}} \tag{2}$$

where $\sum E_{d,i}$ is the total dissipated energy of all the VEDs, E_{sa} is the maximum strain energy of the structure with VEDs, which can be expressed using the summation of the strain energies of the primary structure, E_s, and all of the equipped VEDs, $\sum E_{sd,i}$.

According to Eq. (1), the first term in Eq. (2) can be rewritten as follows when the equivalent damping ratio, $\zeta_{d,i}$, of each VED is set to the constant, ζ, according to the UDR concept:

$$\frac{\sum E_{d,i}}{4\pi \sum E_{sd,i}} = \frac{\sum 4\pi \zeta_{d,i} E_{sd,i}}{4\pi \sum E_{sd,i}} = \frac{4\pi \zeta \sum E_{sd,i}}{4\pi \sum E_{sd,i}} = \zeta \tag{3}$$

Then, defining the second term in Eq. (2) as the stiffness characteristic coefficient, κ, this term can be expressed as follows:

$$\kappa = \frac{\sum E_{sd,i}}{E_s + \sum E_{sd,i}} = \frac{\sum E_{sd,i}}{E_{sa}} \tag{4}$$

Now, the additional damping ratio, ζ_a, can be simplified as follows:

$$\zeta_a = \zeta \cdot \kappa \tag{5}$$

The parameter κ involves the stiffnesses of the VEDs. The details of this part are illustrated later. Eq. (5) shows that the uncoupled effect of the damping and stiffness characteristic parameters of the VEDs is achieved, which can greatly simplify the parameter decision procedure. These two parameters, ζ and κ, are taken into account as key parameters for the seismic retrofit design of structures using VEDs. It should be noted that κ impacts not only the additional damping ratio but also the stiffness of the damped structure. A relatively large stiffness of the damped structure can be beneficial for displacement control. However, a relatively low displacement can limit the energy dissipation capacity of the VEDs. Therefore, there needs to be a balance between the values of ζ and κ. The relevant parameters of VEDs with regard to ζ and κ are discussed below.

2.2. VED parameters

The VEDs are usually connected to the primary structure with braces in series. These two components are installed on the primary structure together. Therefore, both the VED and brace need to be considered for the retrofit design of the structure. The interaction of the VED and brace in the frame structure is illustrated in Fig. 1. The Kelvin model [23,31] is used to represent the VED using a parallel-connected dashpot and spring, and the hysteretic behavior of the VED can be modeled by an elliptical shape under a certain sinusoidal excitation with a frequency, ω. The series-connected VED and brace are considered together as an equivalent viscoelastic damper (EVED) in this study, as shown in Fig. 1, because, except for the value of the corresponding parameters, the hysteretic behavior of the EVED is similar to that of the VED. Due to the series-connected interaction of the VED and brace, the forces of the VED, brace and EVED are equal. This equivalent relationship between the maximum forces of the VED, brace and EVED ($F_{d,max}$, $F_{b,max}$ and $F_{e,max}$) is shown using the dashed line in Fig. 1.

As is shown in Fig. 1, the storage stiffnesses of the VED, K'_d, and the EVED, K'_e, are calculated using the ratios of the forces at the maximum displacement to the corresponding maximum displacements ($u_{d,max}$ and $u_{e,max}$). The relationships between the stiffnesses of the VED and the EVED can be expressed as follows:

$$K'_e = \frac{[(1+\eta_d^2)K'_d + K_b]K'_d K_b}{(K'_d + K_b)^2 + (\eta_d K'_d)^2} \tag{6}$$

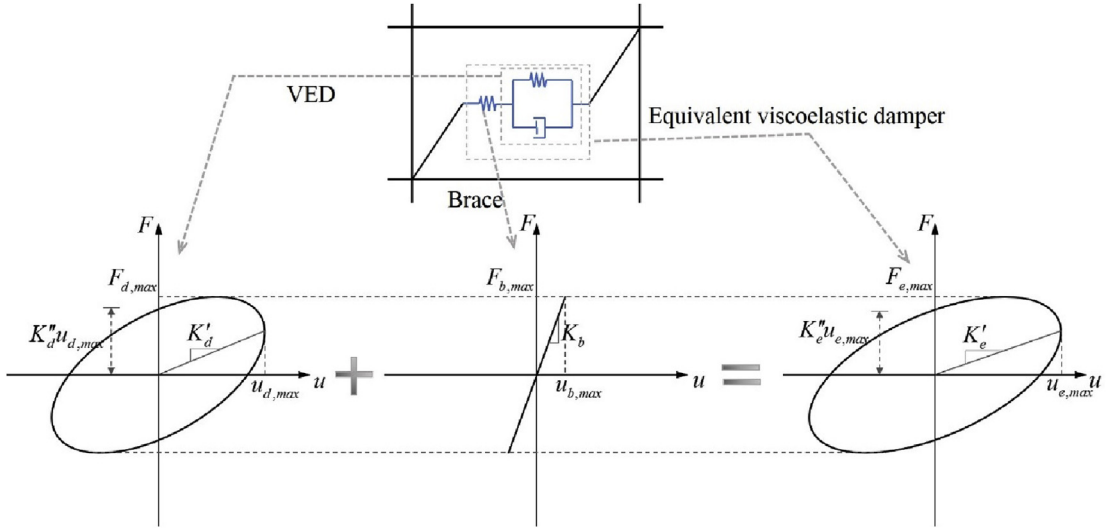

Fig. 1. Interactions and models of the VED and brace.

$$K''_e = \frac{\eta_d K'_d K_b^2}{(K'_d + K_b)^2 + (\eta_d K'_d)^2} \tag{7}$$

where K''_e is the loss stiffness of the EVED, K_b is the stiffness of the brace, $\eta_d = K''_d/K'_d$ denotes the loss factor of the VED, and K''_d is the loss stiffness of the VED. Then, the loss factor of the EVED can be derived as follows:

$$\eta_e = K''_e/K'_e = \frac{\eta_d}{1 + (1 + \eta_d^2)K'_d/K_b} \tag{8}$$

According to Eq. (1), the equivalent damping ratio of the EVED can be calculated as follows:

$$\zeta_e = \frac{E_e}{4\pi E_{se}} = \frac{\pi K''_e u_{e,max}^2}{4\pi K'_e u_{e,max}^2/2} = \frac{\eta_e}{2} \tag{9}$$

where E_e is the energy dissipated by the EVED, and E_{se} is the maximum strain energy of the EVED. Note that the EVED can be regarded as a special VED, and the UDR concept and formulae mentioned in Section 2.1 are also applicable to the EVED (i.e., the equivalent damping ratios, ζ_e, of the EVEDs are equal to the same constant, ζ). It can be seen in Eq. (9) that the value of ζ_e depends on the loss factor, η_e. Hence, the UDR concept for the EVED can be approximately replaced by the uniform loss factor (ULF). This theory can be applied for the simplified design procedure proposed subsequently.

It has been discussed above that the values of ζ and κ for the EVED should be balanced for a reasonable design. The values of ζ and κ for the EVED involve the parameters η_e and K'_e, respectively. According to the studies by Lee et al. [21] and Fu and Kasai [31], for the VED, the typical values of η_d usually range from 1 to 1.4, the values of K'_d/K_s range from 0.1 to 5 and K_b/K_s values ranging from 10 to 30 are also recommended, where K_s is the story stiffness of the primary structure. To obtain a reasonable range for η_e, using Eq. (8) and setting $K_b/K_s = 20$, the values of η_e can be obtained for different values of K'_d/K_s (i.e., $K'_d/K_s = 0.1 - 5$) when the values of η_d are set to 1 and 1.4, as shown in Fig. 2.

It can be seen in Fig. 2 that the values of η_e are between 0.67 and 1.38 for a reasonable parameter set of the VED and brace. Furthermore, η_e is smaller than η_d for a certain damper and decreases with increasing K'_d/K_s for a certain set of η_d and K_b/K_s. In practice, to obtain a better energy dissipation result, a smaller value of K'_d/K_s is usually applied. Moreover, the displacement of the brace is restricted, while the displacement of the VED is encouraged, which means that a relatively large stiffness for the brace and small stiffness for the VED are recommended. Consequently, the condition $K_b/K''_d > 5$ is suggested.

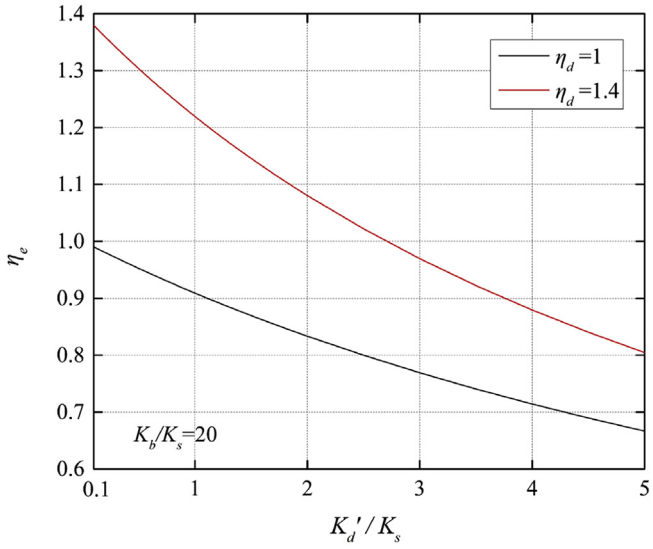

Fig. 2. Relationships between η_e and K'_d/K_s

According to the experiences and theories mentioned above, a reasonable range of η_e can be rounded between 0.7 and 1.3 for a conservative consideration. Similarly, a reasonable range for K'_e/K_s can also be obtained, which is close to K'_d/K_s.

For the seismic retrofit design of structures using VEDs, EVEDs are suggested to consider both the effect of the VEDs and the braces. Once the parameters of the EVED (i.e., η_e and K'_e, etc.) are obtained, the parameters of the VED can be calculated using Eqs. (6)–(8) after setting an appropriate value of K_b/K_s. The detailed design procedures are illustrated below in Section 3.

2.3. Generalized SDOF system

In this study, the widely used frame structure for seismic retrofitting is discussed. To reduce the calculational consumption and simplify the design procedure, the generalized SDOF model is employed to illustrate the frame structure. For a typical frame structure, though the dampers are installed, it is still possible to enter the plastic state of the primary structure under the influence of severe seismic events. Hence, the structural plastic behavior is considered in this study. A multistory frame can usually be simplified to a shear lumped-mass system, which is also called a multi-degree-of-freedom (MDOF) model. According to

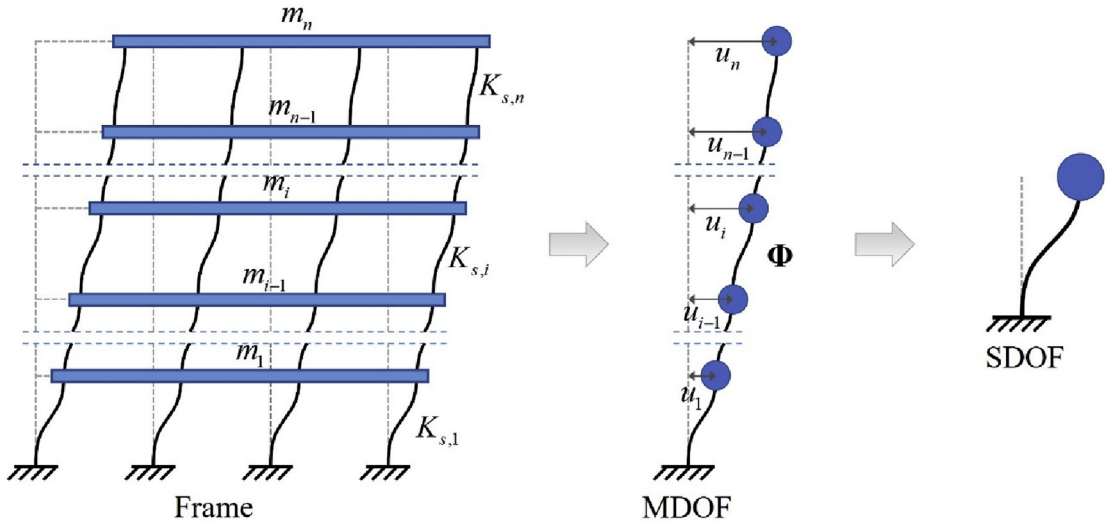

Fig. 3. Transformation of the frame structure to SDOF.

the assumption that the structure can deflect in only one shape throughout the vibration, which is usually the first mode of the structure, the MDOF model can be transformed into a generalized SDOF model, as shown in Fig. 3, where m_i, $K_{s,i}$ and u_i are the mass, stiffness and displacement of story i, respectively. The normalized deflected shape of the MDOF is denoted as a shape vector, $\boldsymbol{\Phi} = [\varphi_1, \cdots, \varphi_i, \cdots, \varphi_n]^T$. Then, the normalized inter-story deflection vector can be denoted as $\boldsymbol{\delta} = [\delta_1, \cdots, \delta_i, \cdots, \delta_n]^T = [\varphi_1, \cdots, \varphi_i - \varphi_{i-1}, \cdots, \varphi_n - \varphi_{n-1}]^T$.

Defining the displacement vector, $\mathbf{u} = [u_1, \cdots, u_i, \cdots, u_n]^T$, of the MDOF as $\mathbf{u} = \boldsymbol{\Phi} q(t)$ on the basis of a constant deflected shape where $q(t)$ denotes the generalized displacement, the motion equation of the generalized SDOF system can be derived as follows [32]:

$$M_{eq}\ddot{q}(t) + C_{eq}\dot{q}(t) + K_{eq}q(t) = -\Gamma_0 M_{eq}\ddot{u}_g(t) \tag{10}$$

where M_{eq} is the equivalent mass of the SDOF system, C_{eq} and K_{eq} are the equivalent damping coefficient and equivalent stiffness of the SDOF system, respectively, Γ_0 is the generalized excitation coefficient, and $\ddot{u}_g$ is the ground acceleration. These corresponding parameters can be calculated as follows:

$$M_{eq} = \sum_{i=1}^{n} m_i \varphi_i^2 \tag{11}$$

$$C_{eq} = 2M_{eq}\zeta_{eq}\cdot\frac{2\pi}{T_{eq}} \tag{12}$$

$$K_{eq} = \sum_{i=1}^{n} K_{s,i}(\varphi_i - \varphi_{i-1})^2 \tag{13}$$

$$\Gamma_0 = \frac{\sum_{i=1}^{n} m_i \varphi_i}{\sum_{i=1}^{n} m_i \varphi_i^2} \tag{14}$$

where $T_{eq} = 2\pi\sqrt{M_{eq}/K_{eq}}$ is the equivalent period, ζ_{eq} is the equivalent damping ratio of the SDOF system, which contains the inherent damping ratio, ζ_0, and the nonlinear hysteretic damping ratio, ζ_s, of the SDOF system.

Actually, some of the parameters above can be obtained through a simple pushover analysis for an elastoplastic primary structure. Performing the pushover analysis, the relationships between the story shear force, Q_i, and the inter-story displacement, $\Delta u_i = u_i - u_{i-1}$ can be obtained first. Then, these $Q_i - \Delta u_i$ curves can be reduced to an $S_a - S_d$ curve, which also graphically represents the transformation of a MDOF system to a SDOF system, as shown in Fig. 4, where S_a and S_d are the spectral acceleration and displacement, respectively. This $S_a - S_d$ curve is also called the capacity spectrum of the elastoplastic primary structure. The corresponding formulae are given as follows:

$$S_a = \frac{Q_1}{\Gamma_0 \sum_{i=1}^{n} m_i \varphi_i} \tag{15}$$

$$S_d = \frac{u_n}{\Gamma_0} \tag{16}$$

The story stiffness, $K_{s,i}$, and the equivalent period, T_{eq}, can be calculated as follows:

$$K_{s,i} = \frac{Q_i}{\Delta u_i} \tag{17}$$

$$T_{eq} = 2\pi\sqrt{\frac{S_d}{S_a}} \tag{18}$$

Using the equivalent bilinear curve of the capacity spectrum, as shown in Fig. 4, ζ_s and ζ_{eq} can be expressed as follows:

$$\zeta_s = \frac{E_p}{4\pi E_s} \tag{19}$$

$$\zeta_{eq} = \zeta_0 + \zeta_s \tag{20}$$

where E_p is the plastic dissipated energy of the primary structure.

When the EVEDs (VEDs and braces) are mounted at the elastoplastic primary structure, considering the UDR concept and adding the stiffness and damping effects of the EVEDs, the equivalent stiffness, K_{eq}^*, and the equivalent damping ratio, ζ_{eq}^*, for the damped SDOF system can be rewritten as follows:

$$K_{eq}^* = \sum_{i=1}^{n} (K_{s,i} + K'_{e,i})(\varphi_i - \varphi_{i-1})^2 \tag{21}$$

$$\zeta_{eq}^* = \zeta_0 + \zeta_s^* + \zeta_a \tag{22}$$

where $K'_{e,i}$ is the storage stiffness of the EVED installed at ith story, and ζ_s^* is the nonlinear hysteretic damping ratio of the damped SDOF system. In this study, the primary structure is considered to install the EVEDs with a proportional stiffness to the primary structure (i.e., value with regard to κ). Hence, the deflected shape of the damped structure can be considered to be almost unchanged compared with the primary structure.

According to Eq. (4), κ can be rewritten as follows on the basis of the unchanged deflected shape:

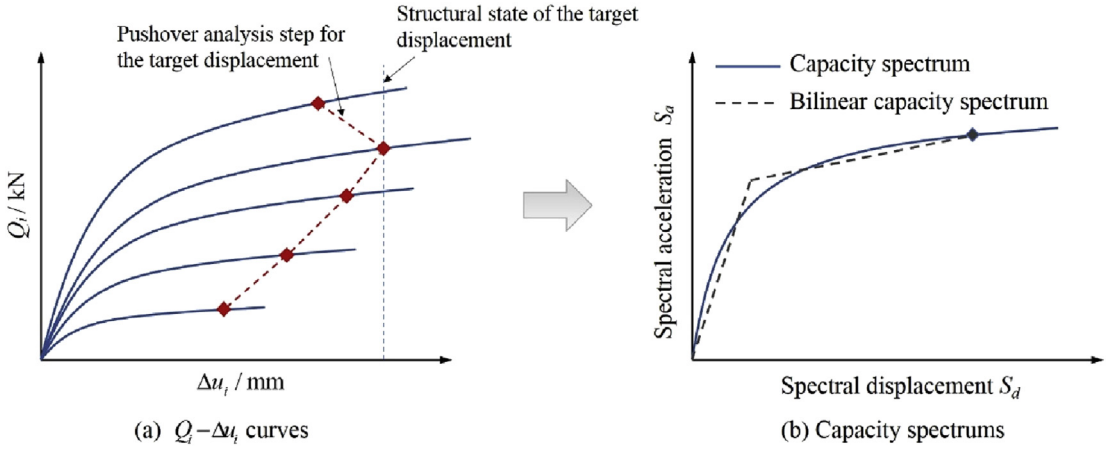

Fig. 4. Transformation of the $Q_i - \Delta u_i$ curves to the capacity spectrum.

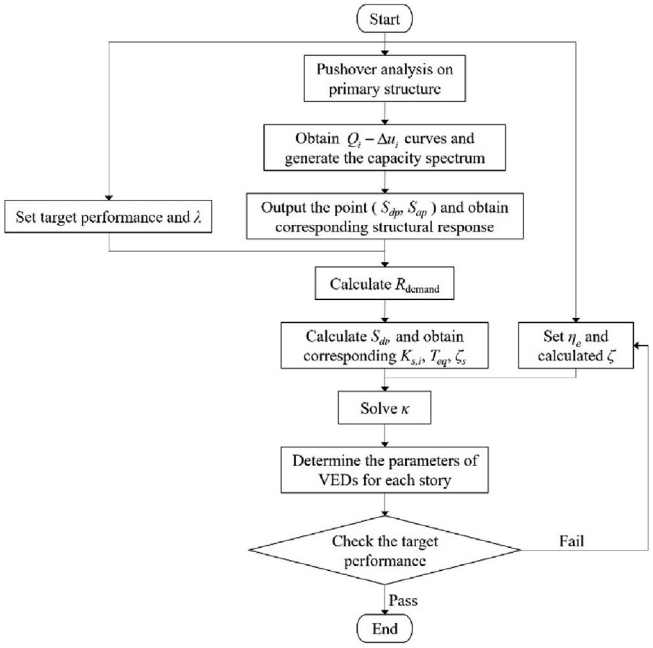

Fig. 5. Flowchart of the seismic retrofit design procedure.

$$\kappa = \frac{\sum E_{sd,i}}{E_s + \sum E_{sd,i}} = \frac{\frac{1}{2}\sum_{i=1}^{n} K'_{e,i}\delta_i^2}{\frac{1}{2}\sum_{i=1}^{n}(K_{s,i} + K'_{e,i})\delta_i^2} = \frac{\sum_{i=1}^{n} K'_{e,i}(\varphi_i - \varphi_{i-1})^2}{\sum_{i=1}^{n}(K_{s,i} + K'_{e,i})(\varphi_i - \varphi_{i-1})^2} \tag{23}$$

Then, the ratio of K_{eq} to K^*_{eq} can be derived as follows:

$$\frac{K_{eq}}{K^*_{eq}} = \frac{\sum_{i=1}^{n} K_{s,i}(\varphi_i - \varphi_{i-1})^2}{\sum_{i=1}^{n}(K_{s,i} + K'_{e,i})(\varphi_i - \varphi_{i-1})^2} = 1 - \frac{\sum_{i=1}^{n} K'_{e,i}(\varphi_i - \varphi_{i-1})^2}{\sum_{i=1}^{n}(K_{s,i} + K'_{e,i})(\varphi_i - \varphi_{i-1})^2} = 1 - \kappa \tag{24}$$

Hence, the equivalent period, T^*_{eq}, of the damped SDOF system can be expressed as follows:

$$T^*_{eq} = T_{eq}\sqrt{\frac{K_{eq}}{K^*_{eq}}} = T_{eq}\cdot\sqrt{1-\kappa} \tag{25}$$

To calculate the equivalent damping ratio, ζ^*_{eq}, of the damped SDOF system, ζ^*_s can be expressed as follows:

$$\zeta^*_s = \frac{E_p}{4\pi(E_s + \sum E_{sd,i})} = \frac{E_p}{4\pi E_s}\cdot\frac{E_s}{(E_s + \sum E_{sd,i})} = \frac{E_p}{4\pi E_s}\cdot\left(1 - \frac{\sum E_{sd,i}}{E_s + \sum E_{sd,i}}\right) = \zeta_s\cdot(1-\kappa) \tag{26}$$

Based on the UDR concept, substituting Eqs. (5) and (26) into Eq. (22), ζ^*_{eq} can be written as follows:

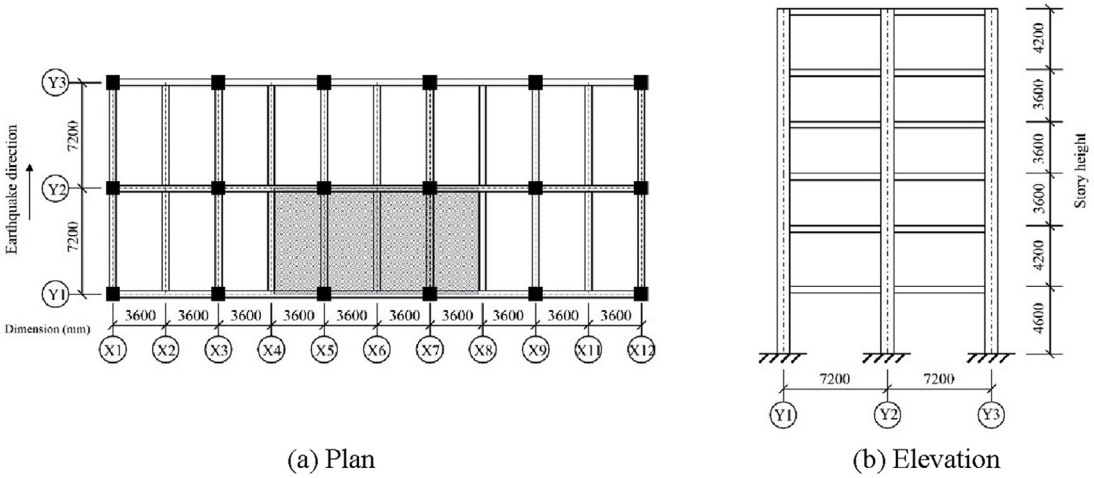

Fig. 6. Diagram of the structural plan and elevation.

Table 1
Dimensions of the structural members and the mass of each story.

Story	Section dimension of column (mm × mm)			Section dimension of beam (mm × mm)			Story mass (t)
	Y1	Y2	Y3	X1-X12	Y1	Y2–Y3	
1	700 × 700	800 × 800	700 × 700	350×600	350×600	350×600	618.3
2	700 × 700	800 × 800	700 × 700	350×500	350×600	350×500	488.2
3	600 × 600	700 × 700	600 × 600	350×600	350×600	350×600	572.0
4	600 × 600	600 × 600	600 × 600	350×600	350×600	350×600	561.8
5	500 × 500	600 × 600	500 × 500	350×600	350×600	350×600	549.9
6	500 × 500	600 × 600	500 × 500	350×600	350×600	350×600	556.9

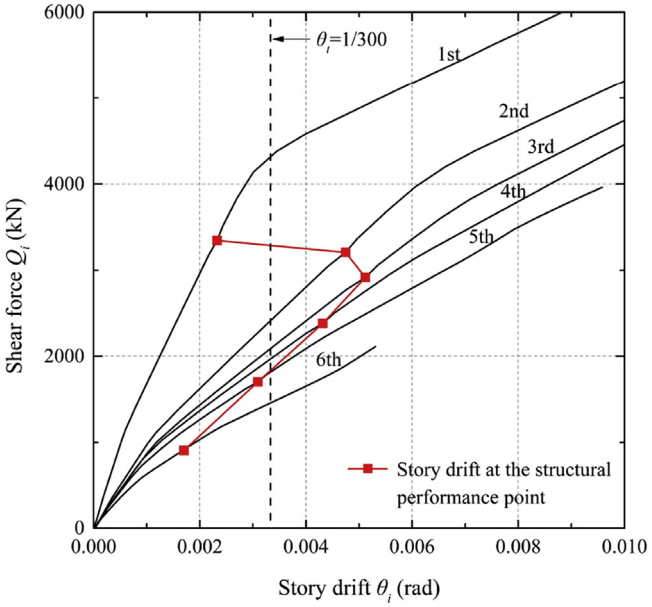

Fig. 7. Relationships between story drift and shear force.

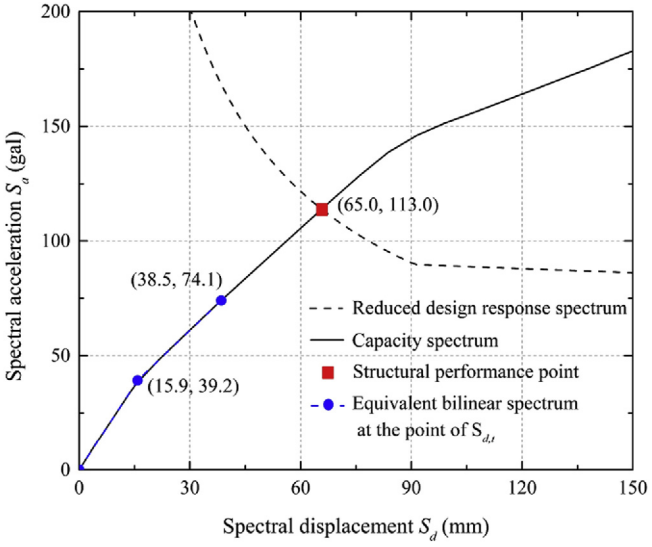

Fig. 8. Capacity spectrums and corresponding performance points.

Table 2
Shear force and story drift at the structural performance point.

Story	1	2	3	4	5	6
Shear force Q_i (kN)	3345	3206	2916	2381	1701	907
Story drift θ_i (rad)	1/430	1/211	1/195	1/232	1/323	1/588

Table 3
Pushover analysis results at the target spectral displacement point.

Story	1	2	3	4	5	6
Shear force Q_i (kN)	2342	2245	2042	1667	1191	635
Story drift θ_i (rad)	1/697	1/347	1/327	1/400	1/581	1/1050
Inter-story displacement Δu_i (mm)	6.6	12.1	11.0	9.0	6.2	4.0
Story stiffness $K_{s,i}$ (kN/mm)	354.8	185.5	185.6	185.2	192.1	158.8

Table 4
Parameters of the EVEDs for each story.

Story	1	2	3	4	5	6
Loss factor $\eta_{e,i}$	0.8	0.8	0.8	0.8	0.8	0.8
Storage stiffness of EVEDs $K'_{e,i}$ (kN/mm)	199.6	104.3	104.4	104.2	108.1	89.3
Maximum damping force of EVEDs $F_{ei,\max}$ (kN)	1687	1617	1471	1201	858	458

$$\zeta^*_{eq} = \zeta_0 + \zeta^*_s + \zeta_a = \zeta_0 + \zeta_s(1-\kappa) + \zeta\cdot\kappa \tag{27}$$

2.4. Determination of the VED parameters

As mentioned above, for the seismic retrofit design of structures using VEDs, the effect of the VEDs and braces together can be considered as EVEDs, which can also be regarded as special VEDs. Hence, based on the UDR concept, ζ and κ can also be seen as two key design parameters to obtain the practical parameters of the EVEDs (i.e., η_e and K'_e, etc.). Then, the parameters of the VEDs can be calculated accordingly. The relationships between the key design parameters and the practical parameters of the EVEDs for each story are discussed in this subsection.

It has been illustrated above that the UDR concept can be seen to be equal to the ULF concept, which means that the loss factor, $\eta_{e,i}$, of the EVEDs for each story can be set to the same constant to fully utilize each damper. Furthermore, since the loss factor is not very sensitive to the frequency dependence property of the VED, and the range for the value of η_e is smaller compared with K'_e/K_s, referring to Section 2.2, a reasonable assumption for the value of η_e is suggested to start the retrofit design of the existing structure in this study. The detailed design procedure is illustrated in Section 3.

The proportional stiffness distribution principle for the EVEDs is suggested to determine the storage stiffnesses of the supplemental EVEDs used for the seismic retrofitting of existing structures. This principle means that the ratios of the storage stiffnesses, $K'_{e,i}$, of the EVEDs to the story stiffness, $K_{s,i}$, are assumed to be the same for each story of the target structure. This principle can lead to an approximately unchanged vibration mode shape after the installation of the VEDs, which is preferable for retrofitting.

Then, based on the unchanged vibration mode shape, Eq. (4) can be rewritten in a vector form as follows:

Table 5
Parameters of the VEDs and braces.

Story		1	2	3	4	5	6
Total parameters of the VEDs and braces for each story	Loss factor $\eta_{d,i}$	0.88	0.88	0.88	0.88	0.88	0.88
	Storage stiffness $K'_{d,i}$ (kN/mm)	202.9	106.1	106.2	105.9	109.9	90.8
	Maximum damping force $F_{di,\max}$ (kN)	1687	1617	1471	1201	858	458
	Stiffness of braces $K_{b,i}$ (kN/mm)	3548	1855	1856	1852	1921	1588
	Number of VEDs	2	2	2	2	2	2
Parameters of each brace and VED for every story	Loss factor $\eta_{d,i}$	0.88	0.88	0.88	0.88	0.88	0.88
	Storage stiffness $K'_{d,i}$ (kN/mm)	101.5	53.1	53.1	53.0	55.0	45.4
	Maximum damping force $F_{di,\max}$ (kN)	844	809	736	601	429	229
	Stiffness of braces $K_{b,i}$ (kN/mm)	1774	928	928	926	961	794

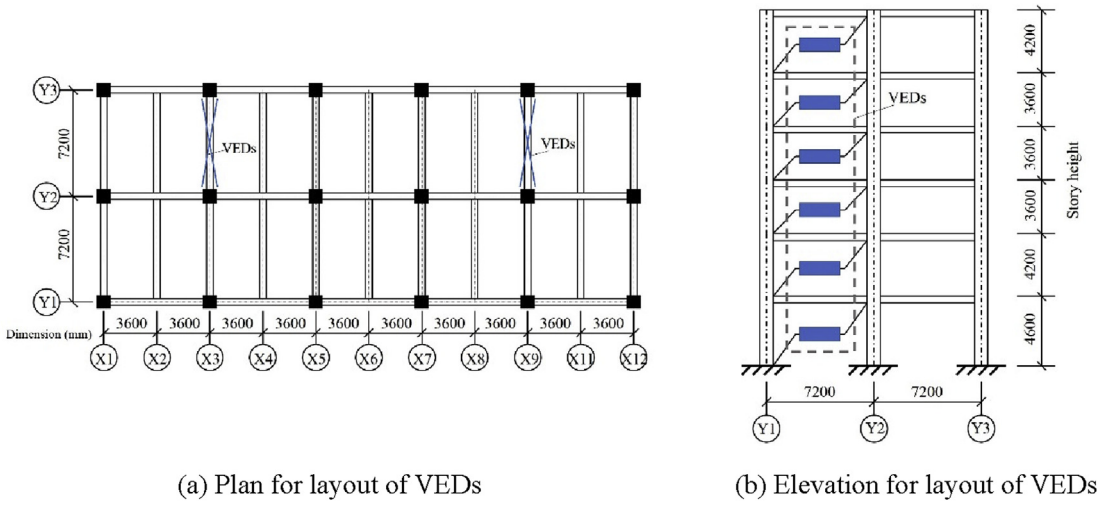

Fig. 9. Layout of the VEDs at the Y-direction frames.

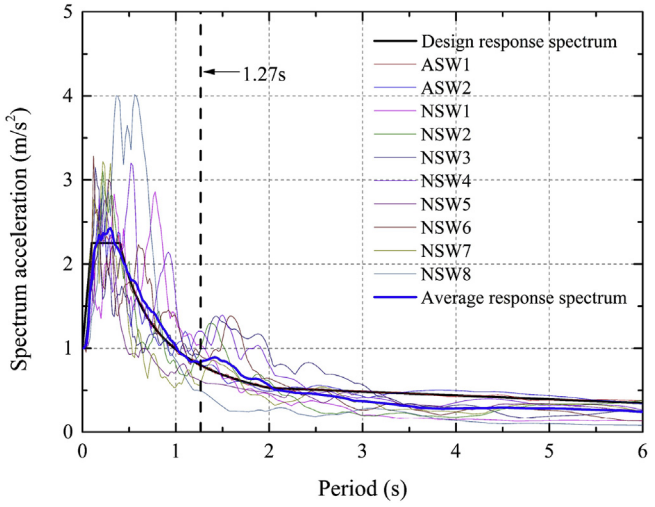

Fig. 10. Diagram of the response spectra.

$$\kappa = \frac{\sum E_{sd,i}}{E_s + \sum E_{sd,i}} = \frac{\frac{1}{2}\sum_{i=1}^{n} K'_{e,i}\delta_i^2}{\frac{1}{2}\sum_{i=1}^{n}(K_{s,i} + K'_{e,i})\delta_i^2} = \frac{\boldsymbol{\delta}^T\cdot\mathbf{K'_e}\cdot\boldsymbol{\delta}}{\boldsymbol{\delta}^T\cdot\mathbf{K_s}\cdot\boldsymbol{\delta} + \boldsymbol{\delta}^T\cdot\mathbf{K'_e}\cdot\boldsymbol{\delta}}$$
$$= \frac{K'_{e,\max}\cdot\boldsymbol{\delta}^T\cdot\tilde{\mathbf{K}}'_{\mathbf{e}}\cdot\boldsymbol{\delta}}{K_{s,\max}\cdot\boldsymbol{\delta}^T\cdot\tilde{\mathbf{K}}_{\mathbf{s}}\cdot\boldsymbol{\delta} + K'_{e,\max}\cdot\boldsymbol{\delta}^T\cdot\tilde{\mathbf{K}}'_{\mathbf{e}}\cdot\boldsymbol{\delta}} \quad (28)$$

where $\mathbf{K'_e} = \mathrm{diag}\{K'_{e,1},\cdots,K'_{e,i},\cdots,K'_{e,n}\}$ is the diagonal storage stiffness matrix of the supplemental EVEDs, $\mathbf{K_s} = \mathrm{diag}\{K_{s,1},\cdots,K_{s,i},\cdots,K_{s,n}\}$ is the diagonal effective story stiffness matrix of the primary structure, $K'_{e,\max}$ and $K_{s,\max}$ are the maximum stiffnesses of the stiffness matrices $\mathbf{K'_e}$ and $\mathbf{K_s}$, respectively, and $\tilde{\mathbf{K}}'_{\mathbf{e}}$ and $\tilde{\mathbf{K}}_{\mathbf{s}}$ denote the normalized versions of $\mathbf{K'_e}$ and $\mathbf{K_s}$, respectively, which also expresses the stiffness distribution modes of the supplemental EVEDs and the primary structure.

Since the proportional stiffness distribution principle is suggested to determine the storage stiffnesses of the supplemental EVEDs, the stiffness distribution mode of the supplemental EVEDs should be equal to that of the primary structure along the story height (i.e., $\tilde{\mathbf{K}}'_{\mathbf{e}} = \tilde{\mathbf{K}}_{\mathbf{s}}$). Then, Eq. (28) can be further derived as follows:

$$\kappa = \frac{K'_{e,\max}\cdot\boldsymbol{\delta}^T\cdot\tilde{\mathbf{K}}'_{\mathbf{e}}\cdot\boldsymbol{\delta}}{K_{s,\max}\cdot\boldsymbol{\delta}^T\cdot\tilde{\mathbf{K}}_{\mathbf{s}}\cdot\boldsymbol{\delta} + K'_{e,\max}\cdot\boldsymbol{\delta}^T\cdot\tilde{\mathbf{K}}'_{\mathbf{e}}\cdot\boldsymbol{\delta}} = \frac{K'_{e,\max}}{K_{s,\max} + K'_{e,\max}} \quad (29)$$

Then, the ratio of storage stiffnesses, $K'_{e,i}$, of the EVEDs for each story to the story stiffness, $K_{s,i}$, can be expressed as follows:

$$\frac{K'_{e,i}}{K_{s,i}} = \frac{K'_{e,\max}}{K_{s,\max}} = \frac{\kappa}{1-\kappa} \quad (30)$$

Clearly, according to the derivations above, the parameter $\kappa/(1-\kappa)$ can be used to proportionally determine the storage stiffnesses of the supplemental EVEDs for each story. The storage stiffness matrix, $\mathbf{K'_e}$, can be written as follows:

$$\mathbf{K'_e} = K'_{e,\max}\tilde{\mathbf{K}}'_{\mathbf{e}} = K_{s,\max}\frac{\kappa}{1-\kappa}\tilde{\mathbf{K}}_{\mathbf{s}} = \frac{\kappa}{1-\kappa}\mathbf{K_s} \quad (31)$$

It should be noted that the proportional stiffness distribution principle is not the optimal pattern to determine the storage stiffnesses of the supplemental EVEDs. However, this principle is relatively simple, effective and easy to implement in practical applications. The optimal distribution pattern of the stiffnesses of the supplemental EVEDs needs further study.

In practice, for seismic retrofit designs using VEDs, if a severely weak story exists in the target structure, the stiffness of the weak story

Table 6
Characteristics of the natural seismic waves.

Name	Year	Moment magnitude	Distance of epicentral (km)	Earthquake name	Station name
NSW1	1976	6.5	33.32	Friuli_Italy-01	Codroipo
NSW2	1942	6.5	56.88	Borrego	El Centro Array #9
NSW3	1966	6.2	17.64	Parkfield	Cholame-Shandon Array #12
NSW4	1978	7.4	24.07	Tabas_Iran	Boshrooyeh
NSW5	1979	6.5	23.17	Imperial Valley-06	Calipatria Fire Station
NSW6	1979	6.5	22.03	Imperial Valley-06	Delta
NSW7	1979	6.5	21.98	Imperial Valley-06	El Centro Array #13
NSW8	1983	6.4	23.78	Coalinga-01	Cantua Creek School

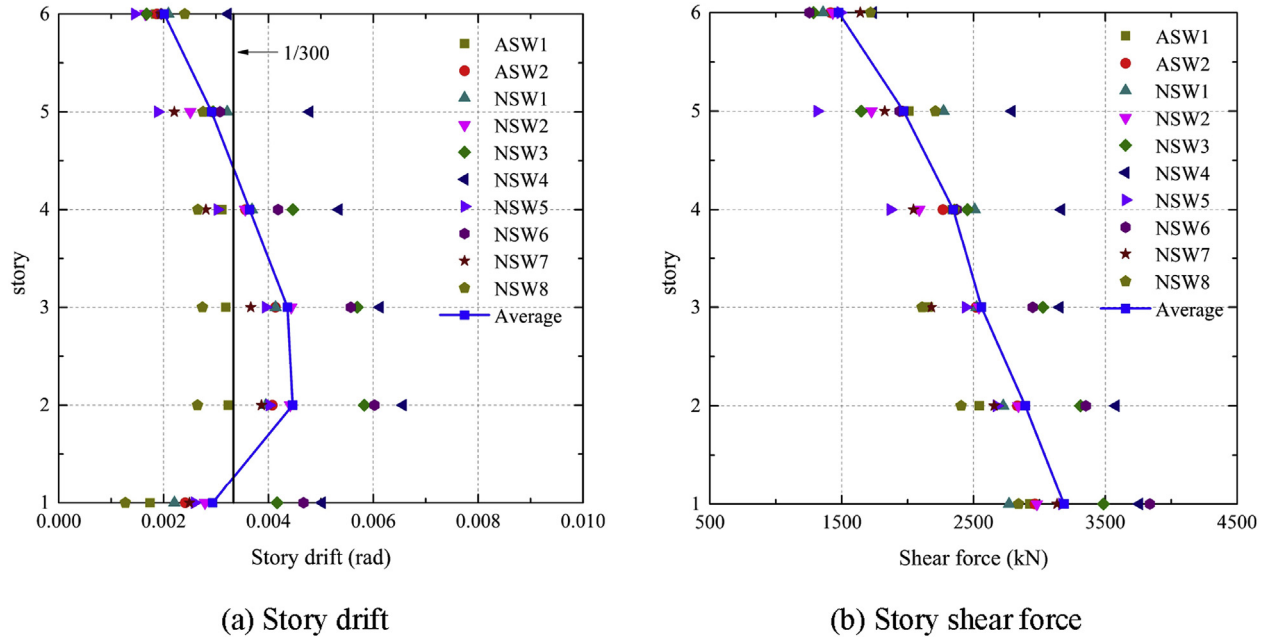

Fig. 11. Story drifts and shear forces of the primary structure under moderate earthquakes.

should be increased first (e.g., by adding braces) and then the storage stiffness of the corresponding VED should be determined. Additionally, for VEDs with closed parameters, the VED types can be merged for convenience. For VEDs with extremely small parameters, the dampers are considered unnecessary and are, thus, removed.

3. UDR-based design procedure

The response reduction ratio is adopted herein to reflect the vibration control effect of the dampers and is used as a design control index in reference to the studies by Shen et al. [33] and Zhang et al. [23]. Then, the stiffness of the VEDs can be directly determined on the basis of the demand performance and without complicated trial calculations of the stiffness [15,21,22]. Combining the theories and concepts mentioned above, the response reduction ratio, R, for the EVEDs can be expressed as follows:

$$R = \frac{S_d\left(T_{eq}^*, \zeta_{eq}^*\right)}{S_{dp}} = \frac{S_d(T_{eq}\cdot\sqrt{1-\kappa}, \zeta_0 + \zeta_s(1-\kappa) + \zeta\cdot\kappa)}{S_{dp}} \tag{32}$$

where S_{dp} is the spectral displacement of the primary structure, and $S_d\left(T_{eq}^*, \zeta_{eq}^*\right)$ is the spectral displacement of the damped structure, which can be further expressed using Eqs. (25) and (27).

Referring to the philosophy of the performance-based design, the seismic retrofit design procedures on the basis of the UDR concept are presented in the following steps, and the corresponding design flowchart is shown in Fig. 5.

1. For seismic retrofit design of existing structures, pushover analysis is performed and then the $Q_i - \Delta u_i$ curves can be obtained. Then, using Eqs. (15) and (16), the $S_a - S_d$ curve can be depicted. According to the capacity spectrum method, the structural performance point, (S_{dp}, S_{ap}), can be found by finding the intersection of the demand spectrum and the capacity spectrum. The story shear force, Q_i, and the inter-story displacement, Δu_i, of the structure at this pushover step of the structural performance point can be obtained accordingly.
2. The target performance (e.g., target roof displacement, $u_{n,t}$, target story drift, θ_t, etc.) of the structure should be set for the design's seismic level. The demand response reduction ratio of the structure can be calculated as follows:

$$R_{\text{demand}} = \frac{\text{Target performance}}{\text{Response of primary structure}} \tag{33}$$

where the response of the primary structure can be the roof displacement, u_n, or ith story drift, θ_i, at the pushover analysis step of the structural performance point. In addition, when the dampers are installed, the design condition, $R \le R_{\text{demand}}/\lambda$, should be satisfied for the seismic retrofit design, where λ is the safety redundancy index for increasing the reliability of the retrofitted structure [34,35].

3. Using Eqs. (32) and (33) and the design condition, $R \le R_{\text{demand}}/\lambda$, the target spectral displacement of the damped structure can be calculated as $S_{d,t} = S_{dp}\cdot R_{\text{demand}}/\lambda$. Then, Q_i and Δu_i for the pushover

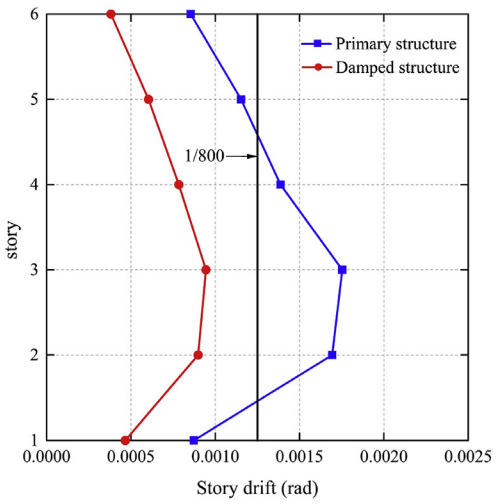

(a) Story drift under frequent earthquake (PGA=0.07 g)

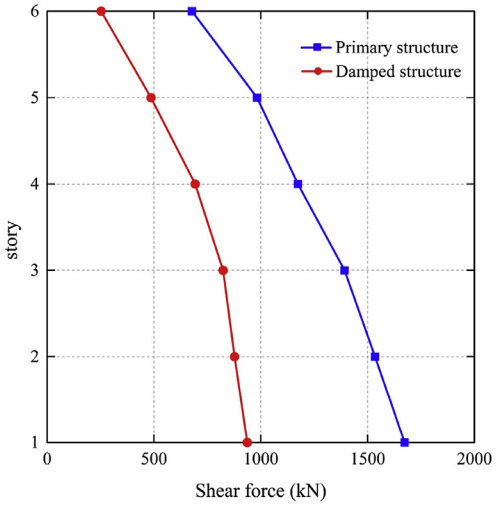

(b) Story shear force under frequent earthquake (PGA=0.07 g)

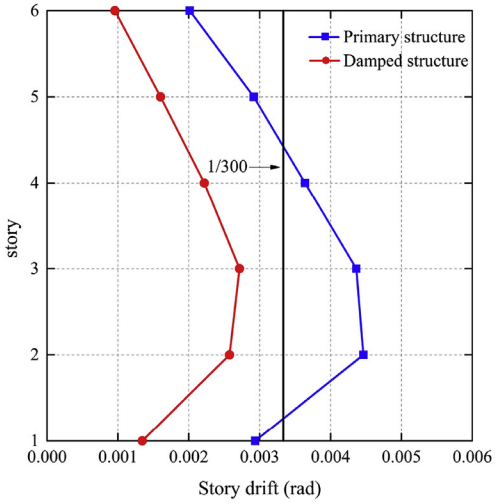

(c) Story drift under moderate earthquake (PGA=0.2 g)

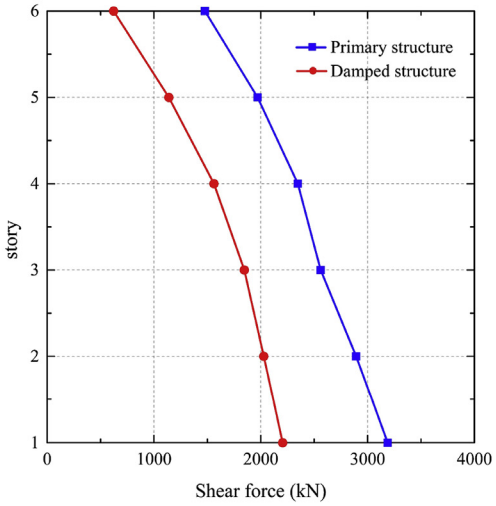

(d) Story shear force under moderate earthquake (PGA=0.2 g)

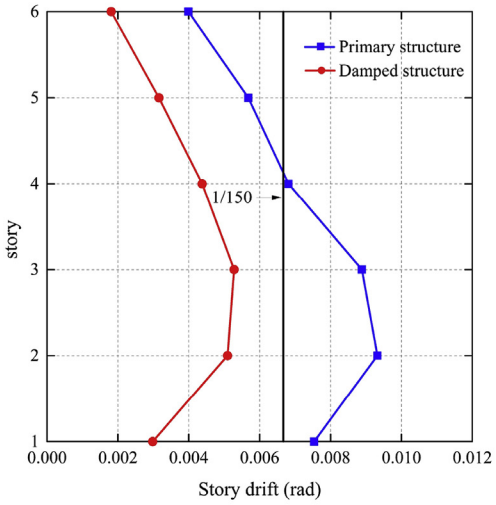

(e) Story drift under rare earthquake (PGA=0.4 g)

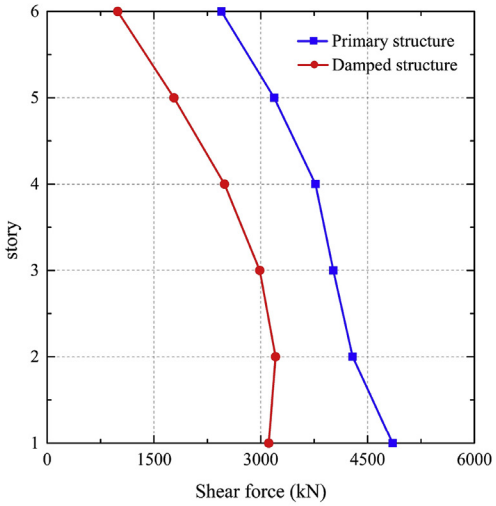

(f) Story shear force under rare earthquake (PGA= 0.4 g)

Fig. 12. Story drifts and shear forces for structure with and without VEDs.

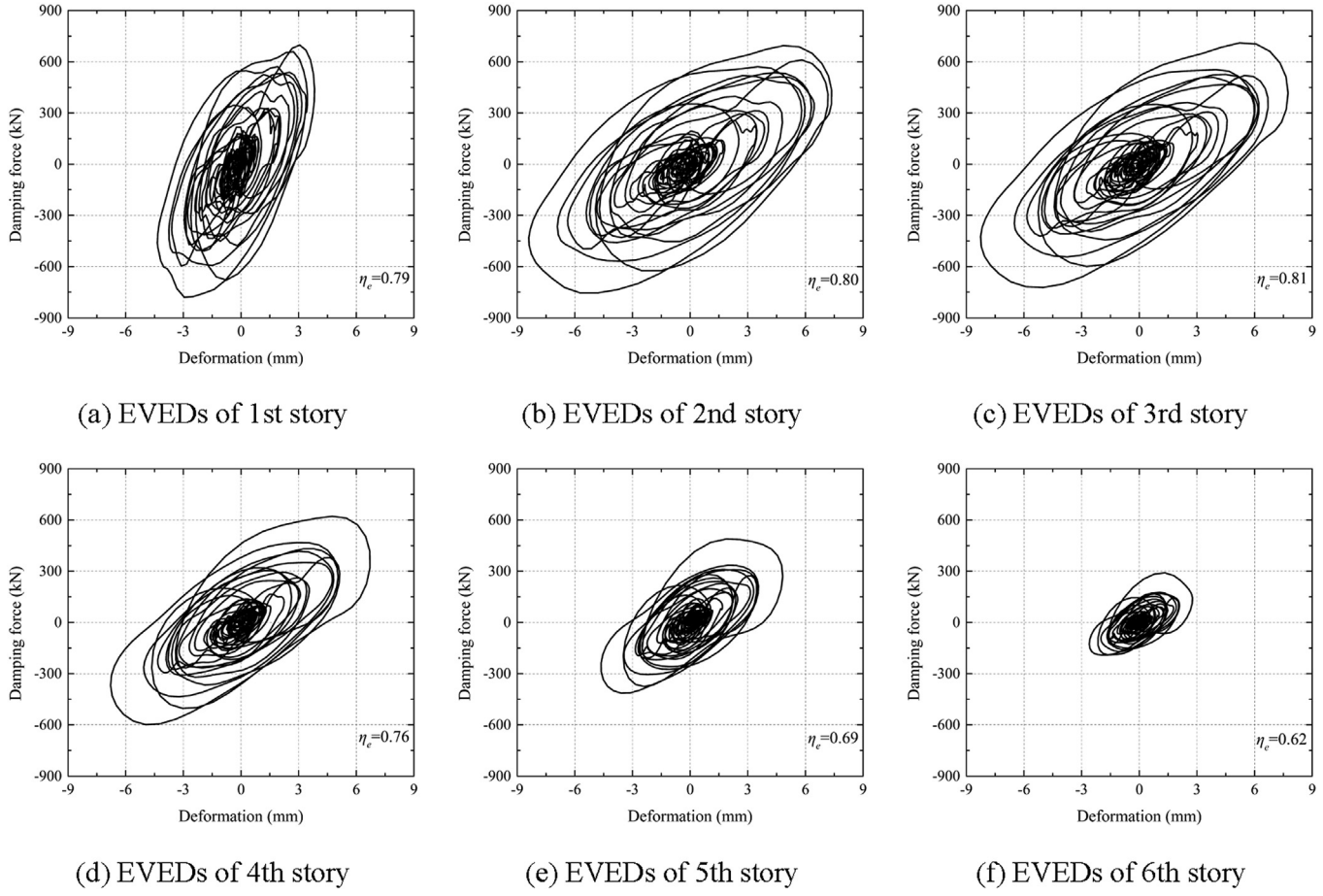

Fig. 13. Hysteretic loops of the EVEDs of each story under a moderate earthquake of the seismic wave NSW 1.

analysis step of $S_{d,t}$ can be obtained, and the corresponding story secant stiffness, $K_{s,i}$, can be calculated to determine the parameter distribution of the EVEDs. For the primary structure, T_{eq} and ζ_s at the point $S_{d,t}$ can also be calculated using the capacity spectrum.

4. The appropriate value of the ULF is selected using the recommended range of η_e for the EVEDs (i.e., 0.7–1.3) in Section 2.3. Due to the frequency dependence of the stiffnesses of the VEDs (stiffness increases with increasing excitation frequency), a relatively small value of η_e can be selected from the recommended range of η_e for a conservative consideration. Then, the value of the UDR ζ for the EVEDs can be calculated according to Eq. (9). Furthermore, the design parameter, κ, can be determined by using Eq. (32) and combining the parameters T_{eq}, ζ_s and $S_{d,t}$ obtained in Step 3 with the design response spectrum.
5. The parameters of the EVEDs for each story can be determined according to the formulae and discussions in Section 2.4. Then, the appropriate value of the stiffness ratio, $K_{b,i}/K_{s,i}$, should be set according to the suggestions in Section 2.2 (i.e., $K_{b,i}/K_{s,i}$ ranges from 10 to 30 and $K_{b,i}/K''_{e,i} > 5$). Using Eqs. (6)–(8), the parameters of the VEDs (i.e., $\eta_{d,i}$, $K'_{d,i}$ and $K''_{d,i}$, etc.) for each story can be determined. In practice, if the design parameters of the dampers in some stories are extremely small, there is no need to add dampers to such floors.
6. The existing structures are equipped with the appropriate VEDs and braces. The seismic performance of the damped structure should be checked using dynamic analysis to verify the retrofit effect. If the target performance for the design's seismic level is satisfied, the design procedure can be stopped. If not, Steps 4–6 should be repeated until the target performance is achieved.

4. Retrofit design example

4.1. Model information

To illustrate the seismic retrofit design method using the VEDs proposed above, a typical six-story RC frame model is considered as an example structure, and the Y-direction of this structure is primarily analyzed. The plan, elevation and calculated earthquake direction of this structure are shown in Fig. 6. The section dimensions (width × height) of the beams and columns are listed in Table 1, and due to an opening in the floor at the shadow area of the 2nd story shown in Fig. 6, the section dimensions of this story are quite different from the other stories. The gravity loads on the floor are expressed as dead and live loads. The values of the dead loads for all the stories are 5.5 kN/m^2, and the values of the live loads for the first five stories and top story are 3 kN/m^2 and 5 kN/m^2, respectively. By considering the total dead loads, half of the live loads and calculating the weight of the structural members, the mass of each story is also determined and given in Table 1. According to the modal analysis results, the fundamental period of this structure is 1.27 s.

This RC frame was designed with the admissible tension method and for a moderate earthquake. According to the Chinese code for the seismic design of buildings [36], the peak ground acceleration (PGA) for the fortification earthquake is 200 gal. The site characteristic period, T_g, and structural inherent damping ratio, ζ_0, are 0.4 s and 0.05, respectively. The design response spectrum is expressed as follows:

$$S_a = \begin{cases} 45(\eta_2 - 0.45)T + 2.025, (0 < T \le 0.1s) \\ 4.5\eta_2, (0.\ 1s < T \le 0.4s) \\ 4.5\eta_2\left(\frac{0.4}{T}\right)^{\gamma}, (0.\ 4s < T \le 2s) \\ 4.5\eta_2 \cdot 0.\ 2^{\gamma} - 4.5\eta_1(T-2), (2 < T \le 6s) \end{cases} \quad (34)$$

$$\gamma = 0.9 + \frac{0.05 - \zeta}{0.3 + 6\zeta} \quad (35)$$

$$\eta_1 = 0.9 + \frac{0.05 - \zeta}{0.3 + 6\zeta} \quad (36)$$

$$\eta_2 = 1 + \frac{0.05 - \zeta}{0.08 + 1.6\zeta} \quad (37)$$

This structure is built as a 3D beam-column element model and the program SAP2000 is adopted. The moment hinges are set at both sides of the beams to simulate the plastic behavior of this element. Accordingly, the P-M-M interactions are considered at both the ends of the columns. The trilinear moment-rotation backbone curves are used for the plastic rotational hinges. A concrete cubic compressive strength of 30 MPa and longitudinal steel bars and stirrups with yielding strengths of 335 MPa are set for the structure.

4.2. Design procedure for the exemplified structure

The pushover analysis is performed on the Y-direction of the primary structure to obtain the performance of this structure, and the corresponding lateral load pattern of the pushover analysis is the first mode distribution. The relationships between the story shear force, Q_i, and the story drift, θ_i, (i.e., $Q_i - \theta_i$ curves) are obtained, as shown in Fig. 7. Then, the corresponding $S_a - S_d$ curve, which is called the capacity spectrum, can be calculated, as shown in Fig. 8. Using the capacity spectrum method, the structural performance point, (S_{dp}, S_{ap}) is found to be (65.0 mm, 113.0 gal). Accordingly, Q_i and θ_i for the pushover analysis step of the structural performance point are listed in Table 2 and marked as red points on the $Q_i - \theta_i$ curves, as shown in Fig. 7. For a moderate earthquake, the target story drift, θ_t, can be set to 1/300. It can be seen in Fig. 7 that several story drifts are beyond the target story drift, θ_t. Hence, a seismic retrofit is needed for this structure and VEDs are used to mitigate the seismic response.

The safety redundancy index, λ, is set to 1.1 for this structure [34,35]. Using Eq. (33), the demand response reduction ratio, R_{demand}, is calculated as 0.65. Then, the target spectral displacement is obtained as $S_{d,t} = \frac{65.0 \times 0.65}{1.1} = 38.5$mm. Accordingly, Q_i and θ_i for the pushover analysis step of $S_{d,t}$ can also be found from the $Q_i - \theta_i$ curves. Then, the inter-story displacement, Δu_i, can be obtained. In addition, the corresponding secant stiffness, $K_{s,i}$, can be calculated using Eq. (17). These values are listed in Table 3. Using the equivalent bilinear capacity spectrum at the point $S_{d,t}$, the nonlinear hysteretic damping ratio, ζ_s, and the equivalent period, T_{eq}, can be calculated as 0.075 and 1.43 s, respectively.

To mitigate the seismic response and meet the target performance, VEDs with matching braces are installed at the primary structure. These two components are together called the EVED, as mentioned above. Based on the UDR concept, the ULF is recommended to be $\eta_e = 0.8$ for the equipped EVEDs according to the suggestion above. Moreover, the UDR for the EVEDs can be calculated as $\zeta = 0.4$. Then, using Eq. (32) and combining the value of ζ_s and T_{eq} with the design response spectrum expressed by Eqs. (34)–(37), the stiffness characteristic coefficient, κ, can be determined as 0.36 for the EVEDs. For the damped structure, the equivalent period, T^*_{eq}, and damping ratio, ζ^*_{eq}, are calculated as 1.14 s and 0.242, respectively.

According to the value of κ, the storage stiffness, $K'_{e,i}$, of the EVEDs can be obtained using Eq. (31). Then, the maximum damping force of the EVEDs, $F_{ei,\max}$, can be calculated using $F_{ei,\max} = \sqrt{{K'_{e,i}}^2 + {K''_{e,i}}^2} \cdot \Delta u_i$. The parameters of the EVEDs are listed in Table 4. In this study, the ratio $K_{b,i}/K_{s,i}$ is set to 10. Then, the parameters of the VEDs can be calculated according to Eqs. (6)–(8). The maximum damping forces of the VEDs, $F_{di,\max}$, are equal to $F_{ei,\max}$, as mentioned above. Two VEDs are equipped for each story of the primary structure. The total parameters for the VEDs and braces of each story, and the parameters for each VED and brace, are listed in Table 5. The layout of these two dampers at the Y-direction frames is shown in Fig. 9.

To verify the seismic retrofit effect of the structure using VEDs, a time history analysis is conducted and the dynamic responses of the structure with and without VEDs are compared. Matching the design response spectrum, ten seismic waves are used for the dynamic analysis according to the Chinese code for the seismic design of buildings [36]. These ten waves contain two artificial seismic waves (ASW 1 and ASW 2) and eight natural seismic waves (NSW 1–8) [37,38]. The corresponding response spectra of these waves, and the normalized design response spectrum, are depicted in Fig. 10. It can be seen that the average response spectrum of these ten waves matches well with the design response spectrum, as shown in Fig. 10. Table 6 lists the characteristics of the natural seismic waves.

The time history analysis is first performed under a moderate earthquake (design earthquake intensity) for the primary structure. The PGA for a moderate earthquake is 200 gal. The story drifts and story shear forces under the dynamic analyses of the moderate earthquakes are shown in Fig. 11. It can be seen that the average story drifts for several stories under the moderate earthquakes are beyond the target story drift of 1/300. Then, the VEDs with the parameters listed above are installed at suitable places on the primary structure using the corresponding braces.

For the damped structure, time history analyses are performed under different seismic levels. The PGAs of frequent and rare earthquakes are 70 gal and 400 gal, respectively. Accordingly, the target drifts of frequent and rare earthquakes are set to 1/800 and 1/150, respectively. In addition, for comparison, the dynamic analyses under different seismic levels are also conducted on the primary structure. Under different seismic levels, the average story drifts and shear forces for the structure with and without VEDs are presented in Fig. 12. The results show that the displacement and shear force responses of the structure are effectively reduced and that the target performances are satisfied under different seismic levels, which verifies that the parameters determined using the UDR concept are reasonable.

As mentioned above, in this study, the VED and its corresponding brace are represented by an EVED to consider the effects of both of these components. Under a moderate earthquake, the hysteretic loops of the EVEDs for each story are checked for seismic wave NSW 1, as shown in Fig. 13. The loss factors of the EVEDs for each story are also expressed in Fig. 13. It can be seen that the loss factors of the EVEDs are approximately equal for every story. The full hysteretic loops show effective energy dissipation of the EVEDs, and the approximately uniform loss factors validate the UDR concept.

5. Conclusions

A simple seismic retrofit design method for elastoplastic structures using VEDs is proposed on the basis of the uniform damping ratio concept. The uniform damping ratio concept gives rise to design formulas for damped structures with VEDs. The parameter distribution principle is also established. A six-story RC frame is adopted to illustrate the seismic retrofit design procedure. Our conclusions are summarized as follows:

1. The uniform damping ratio concept can make full utilization of dampers and lead to uncoupled stiffness and damping characteristic parameters of VEDs, making the design of VEDs simple and convenient.
2. The response reduction ratio is employed as the design target to avoid a complicated trial calculation process in the proposed design

procedure.

3. The seismic response of the instance structure can be mitigated as expected when VEDs are equipped using the proposed design procedure, which proves that the UDR-based design method is feasible and reasonable.

Acknowledgments

This study was supported by the National Natural Science Foundation of China (No. 51978525 & 51778490), the Key Program for International S&T Cooperation Projects of China (No. 2016YFE0127600), the Fundamental Research Funds for the Central Universities (No. 22120180064), and the Natural Science Foundation of Shandong Province (No. ZR2018BEE033).

References

[1] Soong TT, Spencer BF. Supplemental energy dissipation: state-of-the-art and state-of-the practice. Eng Struct 2002;24(3):243–59.
[2] Constantinou MC, Soong TT, Dargush GF. Passive energy dissipation systems for structural design and retrofit. Buffalo (NY): Research Foundation of the State University of New York and the Multidisciplinary Center for Earthquake Engineering Research; 1998.
[3] Luo H, Zhang RF, Weng DG. Mitigation of liquid sloshing in storage tanks by using a hybrid control method. Soil Dyn Earthq Eng 2016;90:183–95.
[4] Zhang RF, Zhao ZP, Pan C. Influence of mechanical layout of inerter systems on seismic mitigation of storage tanks. Soil Dyn Earthq Eng 2018;114:639–49.
[5] Pan C, Zhang RF, Luo H, Li C, Shen H. Demand-based optimal design of oscillator with parallel-layout viscous inerter damper. Struct Control Health Monit 2018;25(1):e2051.
[6] Pan C, Zhang RF. Design of structure with inerter system based on stochastic response mitigation ratio. Struct Control Health Monit 2018;25(6):e2169.
[7] Chen QJ, Zhao ZP, Zhang RF, Pan C. Impact of soil–structure interaction on structures with inerter system. J Sound Vib 2018;433:1–15.
[8] Xu ZD, Wang DX, Shi CF. Model, tests and application design for viscoelastic dampers. J Vib Control 2011;17(9):1359–70.
[9] Dargush GF, Sant RS. Evolutionary aseismic design and retrofit of structures with passive energy dissipation. Earthq Eng Struct Dyn 2005;34(13):1601–26.
[10] Guneyisi EM, Azez I. Seismic upgrading of structures with different retrofitting methods. Earthq Struct 2016;10(3):589–611.
[11] Shen KL, Soong TT, Chang KC, Lai ML. Seismic behavior of reinforced-concrete frame with added viscoelastic dampers. Eng Struct 1995;17(5):372–80.
[12] Lai ML, Chang KC, Soong TT, Hao DS, Yeh YC. Full -scale viscoelastically damped steel frame. J Struct Eng 1995;121(10):1443–7.
[13] Zhang RH, Soong TT. Seismic design of viscoelastic dampers for structural applications. J Struct Eng 1992;118(5):1375–92.
[14] Christopoulos C, Montgomery M. Viscoelastic coupling dampers (VCDs) for enhanced wind and seismic performance of high-rise buildings. Earthq Eng Struct Dyn 2013;42(15):2217–33.
[15] Mazza F, Vulcano A. Control of the earthquake and wind dynamic response of steel-framed buildings by using additional braces and/or viscoelastic dampers. Earthq Eng Struct Dyn 2011;40(2):155–74.
[16] Symans MD, Charney FA, Whittaker AS, Constantinou MC, Kircher CA, Johnson MW, et al. Energy dissipation systems for seismic applications: current practice and recent developments. J Struct Eng 2008;134(1):3–21.
[17] Lewandowski R, Slowik M, Przychodzki M. Parameters identification of fractional models of viscoelastic dampers and fluids. Struct Eng Mech 2017;63(2):181–93.
[18] Lewandowski R, Bartkowiak A, Maciejewski H. Dynamic analysis of frames with viscoelastic dampers: a comparison of damper models. Struct Eng Mech 2012;41(1):113–37.
[19] Singh MP, Chang TS. Seismic analysis of structures with viscoelastic dampers. J Eng Mech 2009;135(6):571–80.
[20] Chang TS, Singh MP. Mechanical model parameters for viscoelastic dampers. J Eng Mech 2009;135(6):581–4.
[21] Lee KS, Fan CP, Sause R, Ricles J. Simplified design procedure for frame buildings with viscoelastic or elastomeric structural dampers. Earthq Eng Struct Dyn 2005;34(10):1271–84.
[22] Mazza F, Vulcano A. Displacement-based design procedure of damped braces for the seismic retrofitting of rc framed buildings. Bull Earthq Eng 2015;13(7):2121–43.
[23] Zhang L, Su MZ, Zhang C, Shen H, Islam MM, Zhang RF. A design method of viscoelastic damper parameters based on the elastic-plastic response reduction curve. Soil Dyn Earthq Eng 2019;117:149–63.
[24] Manual JSSI. Design and construction manual for passively controlled buildings. Tokyo, Japan: Japan Society of Seismic Isolation; 2007. [in Janpanese)].
[25] Tchamo JM, Ying Z. An alternative practical design method for structures with viscoelastic dampers. Earthq Eng Eng Vib 2018;17(3):459–73.
[26] Fujita K, Moustafa A, Takewaki I. Optimal placement of viscoelastic dampers and supporting members under variable critical excitations. Earthq Struct 2010;1(1):43–67.
[27] Zhao XF, Wang SG, Du DS, Liu WQ. Optimal design of viscoelastic dampers in frame structures considering soil-structure interaction effect. Shock Vib 2017;2017:9629083.
[28] Shmerling A, Levy R, Reinhorn AM. Seismic retrofit of frame structures using passive systems based on optimal control. Struct Control Health Monit 2018;25:e2038.
[29] Zhang RF, Wang C, Pan C, Shen H, Ge Q, Zhang L. Simplified design of elastoplastic structures with metallic yielding dampers based on the concept of uniform damping ratio. Eng Struct 2018;176:734–45.
[30] Clough RW, Penzien J. Dynamics of structures. second ed. New York: McGraw-Hill; 1993.
[31] Fu YM, Kasai K. Comparative study of frames using viscoelastic and viscous dampers. J Struct Eng 1998;124(5):513–22.
[32] Chopra AK. Dynamics of structures: theory and applications to earthquake engineering. Englewood Cliffs(NJ): Prentice; 1995.
[33] Shen H, Zhang RF, Weng DG, Gao C, Luo H, Pan C. Simple design method of structure with metallic yielding dampers based on elastic–plastic response reduction curve. Eng Struct 2017;150:98–114.
[34] Hao LF, Zhang RF, Jin K. Direct design method based on seismic capacity redundancy for structures with metal yielding dampers. Earthq Eng Struct Dyn 2018;47(2):515–34.
[35] Hao LF, Zhang RF. Structural safety redundancy-based design method for structure with viscous dampers. Struct Eng Mech 2016;59(5):821–40.
[36] GB 50011-2010. Code for seismic design of buildings. Beijing: the Ministry of Housing and Urban-Rural Construction of the People's Republic of China; 2010.
[37] Pan C, Zhang RF, Luo H, Shen H. Target-based algorithm for baseline correction of inconsistent vibration signals. J Vib Control 2018;24(12):2562–75.
[38] Pan C, Zhang RF, Luo H, Shen H. Baseline correction of vibration acceleration signals with inconsistent initial velocity and displacement. Adv Mech Eng 2016;8(10).